Original Article

Loss of ARID1A Promotes Hepatocellular Carcinoma Progression via Up-regulation of MYC Transcription

Yao Xiao[1,2,3], Guodong Liu[1,2], Xiwu Ouyang[1], Denggao Zai[1], Jixiang Zhou[1], Xiaoli Li[1], Qi Zhang[1] and Jie Zhao[4*]

[1]Department of General Surgery, Xiangya Hospital, Central South University, Changsha, Hunan, China; [2]National Clinical Research Center for Geriatric Disorders, Xiangya Hospital, Central South University, Changsha, Hunan, China; [3]International Joint Research Center of Minimally Invasive Endoscopic Technology Equipment & Standards, Changsha, Hunan, China; [4]Department of General Surgery, Sir Run Run Shaw Hospital, School of Medicine, Zhejiang University, Hangzhou, Zhejiang, China

Abstract

Background and Aims: AT-rich interactive domain-containing protein 1A (ARID1A) is frequently mutated or deficient in hepatocellular carcinoma (HCC). However, the role of ARID1A in HCC remains unclear. Therefore, the biological role of ARID1A in HCC was evaluated and a potential mechanism was investigated. ***Methods:*** *Arid1a* was knocked out in the livers of mice using the CRISPR/Cas9 system delivered by hydrodynamic tail vein injection. The development of HCC was observed in different mouse models. The correlation of ARID1A and prognosis in patients with HCC was analyzed using cBioPortal. The effect of ARID1A on cell proliferation was assessed by MTT assay following the manipulation of candidate genes. ***Results:*** ARID1A deficiency alone did not cause HCC in mice, but knockout of *ARID1A* accelerated liver tumorigenesis in response to diethylnitrosamine (DEN) or when a combination knockout of phosphatase and tensin homolog (*Pten*) plus tumor protein P53 (*p53*) was introduced. *ARID1A* mutations were associated with a poorer prognosis in HCC patients. The mRNA level of MYC was significantly higher in patients with an *ARID1A* mutation compared to those without a mutation. Ectopic expression of ARID1A inhibited HCC cell proliferation. ARID1A knockout increased HCC cell growth and resulted in disruptions to DNA damage repair and apoptosis following radiation stress. Furthermore, mechanistic studies revealed that ARID1A inhibited the proliferation of HCC cells via transcriptional down-regulation of MYC. ***Conclusions:*** These results describe ARID1A as a tumor suppressor in the liver. A deficiency in ARID1A predicts worse survival in HCC patients and promotes HCC progression via up-regulation of MYC transcription.

Introduction

Hepatocellular carcinoma (HCC) is one of the most common types of malignant digestive system tumors and is associated with a high mortality rate.[1] Occurrence and development of HCC involves the alteration of many genes and signaling pathways, but its pathogenic mechanism has not been fully elucidated.[2] To gain a comprehensive understanding of the genetic alterations that occur during HCC initiation, many researchers have analyzed the HCC genome using whole-genome sequencing strategies.[3,4] To date, several genes, including *telomerase reverse transcriptase* (*TERT*), *tumor protein P53* (*p53*), *AT-rich interactive domain 1A* (*ARID1A*), *cyclin dependent kinase inhibitor 2A* (*CDKN2A*), *catenin beta 1* (*CTNNB1*), *axin 1* (*AXIN1*), and *cyclin D1* (*CCND1*), among others, have been shown to be related to HCC.[5]

ARID1A, its encoding gene located on chromosome 1p36.11, represents a subunit of the switch/sucrose non-fermentable (SWI/SNF) chromatin remodeling complex.[6] Chromatin remodeling complexes modify chromatin structures and regulate the transcription of genes to control various cellular processes.[7] Inactivating mutations in ARID1A have been identified in a wide variety of cancers, suggesting that it functions as a tumor suppressor.[8] However, its anticancer mechanisms of action in HCC are not fully understood.

MYC is a transcription factor encoded by the *c-MYC* gene that regulates an estimated 15% of genes in the human genome.[9] MYC is an oncoprotein that contributes to the ma-

lignancy of many aggressive cancers.[10] The *c-MYC* locus is the most frequently amplified locus across all human cancers, leading to MYC overexpression.[11] MYC is frequently overexpressed in patients with HCC[12–14] and experimental overexpression of MYC in the livers of mice can lead to the development of HCC.[15]

In this study, the role of ARID1A in HCC progression was investigated. Using *in vitro* cell models and *in vivo* mouse models, ARID1A deficiency was shown to accelerate the development and progression of liver cancer. Furthermore, mechanistic studies revealed that ARID1A inhibits proliferation in HCC cells via the down-regulation of *c-MYC* transcription.

Methods

Cell culture

The Bel7404 cell line was a gift from Professor Cang (Zhejiang University, Hangzhou, China). The Huh7 and HepG2 cell lines were purchased from American Type Culture Collection (ATCC, Manassas, VA, USA). Huh7 and Bel7404 cells were grown in Roswell Park Memorial Institute (RPMI) 1640 media (Invitrogen, Grand Island, NY, USA) supplemented with 10% fetal bovine serum, 1% penicillin/streptomycin and 1% glutamine in an incubator maintained at 37°C with 5% CO_2. HepG2 cells were cultured in Dulbecco's modified Eagle's medium (DMEM) (Corning Life Science, Corning, NY, USA).

Plasmid and lentivirus

The clustered regularly interspaced short palindrome repeats/CRISPR-associated protein 9 (CRISPR/Cas9) system (PSpCas9(BB)-2A-Puro; PX459) was purchased from Addgene (Watertown, MA, USA). Knockout cells were generated by transfecting the cells with CRISPR/Cas9 using Lipofectamine™ 2000 (Invitrogen), according to a previous report.[16] Individual cells were selected to generate monoclonal cell lines (Bel7404 ARID1A KO-1 and KO-2). LentiCRISPR v2-sgARID1A (Addgene) and pLenti-puro-ARID1A (Addgene) lentiviral vectors were used to knockout and overexpress ARID1A, respectively. To generate stable transfectants, the lentiviral vector, the psPAX2 packaging plasmid (10 µg), and the pMD2.G envelope plasmid (10 µg) were transfected into 293T cells using the standard calcium phosphate transfection method. Lentivirus soups were collected and concentrated by density gradient after 48 h for immediate use, or were frozen at −80°C for later use.

In vivo experiment and hydrodynamic tail vein injection

The animal experiment closely adhered to the Zhejiang University guide for the care and use of laboratory animals. For DEN treatment, 14 day-old male C57BL/6 mice were administered with a single intraperitoneal injection of DEN (25 µg/g body weight). A pX459 vector co-expressing an sgRNA targeting *Arid1a*, *Pten* or *p53* was cloned. Vectors for hydrodynamic tail vein injections were prepared using the EndoFreeMaxi Kit (Qiagen, Hilden, Germany). For hydrodynamic liver injection, plasmid DNA suspended in 2 mL saline was injected into 8 week-old male C57BL/6 mice via the tail vein within 6–7 sec. The amount of injected DNA was 60 µg for sg*Arid1a*, and 60 µg each for sg*Arid1a*+sg*Pten*+sg*p53*. An equal amount of pX459 was used as a control for each experiment.

Western blot

Cells were lysed in NETN lysis buffer and 30 µg total protein was run on a gel using sodium dodecyl sulfate polyacrylamide gel electrophoresis. After electrophoresis, proteins were transferred onto a polyvinylidene fluoride membrane (Millipore, Burlington, MA, USA). After blocking for 1 h, membranes were rinsed with Tris-buffered saline with Tween-20 (TBST) three times and incubated in the corresponding primary antibody at 4°C overnight (antibodies listed in Supplementary Table 2). The membranes were then rinsed three times with TBST and incubated with secondary antibodies. Finally, membranes were incubated with an enhanced chemiluminescence system (ThermoFisher Scientific, Waltham, MA, USA). The bands were detected by ChemiDoc XRS Image System (Bio-Rad Laboratories, Hercules, CA, USA).

Immunohistochemistry

Tissues were fixed in 4% paraformaldehyde (PFA) and embedded in paraffin. Paraffin sections (4 µm) were dewaxed by xylene and rehydrated in decreasing concentrations of ethanol. Epitope retrieval was performed in 10 mM citrate buffer (pH 6.0) at 95°C for 20 m in a microwave oven. Endogenous peroxidase activity was blocked for 10 min by 0.3% H_2O_2 in phosphate-buffered saline (PBS). Tissue sections were incubated with antibodies overnight (shown in Supplementary Table 2). Next, the sections were incubated with a diluted biotinylated goat anti-rabbit IgG antibody (Vector Laboratories, Burlingame, CA, USA) for 30 m at room temperature. Chromogenic reactions were carried out according to the protocols provided in the ImmPACT™ DAB kit (Vector Laboratories).

Immunofluorescence (IF)

Cells were plated and grown on glass slides, washed with PBS, and fixed with 4% PFA for 15 m. Cells were then washed again with PBS and treated with 0.2% Triton X-100 (ThermoFisher Scientific) in PBS for 10 m to permeabilize the cells. After washing with PBS again, the cells were blocked with 2% bovine serum albumin (ThermoFisher Scientific) in PBS at room temperature for 1 h, then incubated with primary antibodies (Supplementary Table 2) at 4°C overnight. Cells were washed once with PBS, then incubated with secondary IF-specific antibodies at room temperature for 1 h. The cells were observed under a laser scanning confocal microscope (LSM710; Zeiss, Oberkochen, Germany). 4′,6-diamidino-2-phenylindole (DAPI) and F-actin were used as staining controls.

Quantitative reverse-transcription polymerase chain reaction (qPCR)

TRIzol reagent (Invitrogen) was used to extract the total RNA from cells, and 2 µg of total RNA was used for reverse transcription. The Bio-Rad CFX96 system was used to conduct the qPCR and calculate the expression of mRNA. Data were normalized to glyceraldehyde 3-phosphate dehydrogenase (GAPDH) and relative expression was assessed using the ΔΔCt method. All primers used are shown

in Supplementary Table 3. Experiments were performed in triplicate.

3-(4,5-dimethylthiazol-2-yl)-2,5-diphenyl-2H-tetra-zolium bromide (MTT) cell viability assay

HCC cells were plated in 24-well plates at a density between 2×10^3 and 5×10^3 cells per well. After treatment, culture media was removed and 500 µL of MTT (0.5 mg/mL) per well was added and cells were incubated at 37°C with 5% CO_2 for 1 h. The absorbance at 570nm was detected. Cell viability was calculated using the formula: [optical density (OD; sample) − OD (blank)] / [OD (control) − OD (blank)]. Experiments were repeated at least three times.

Analysis of The Cancer Genome Atlas (TCGA) data

The subset of data from TCGA Liver Hepatocellular Carcinoma (source data from Genome Data Analysis Centre [GDAC] Firehose) of the cbioportal.org website was analyzed. Specifically, on the home page of the website, "liver" was selected, then "Liver Hepatocellular Carcinoma (TCGA, Firehose Legacy)". "Explore Selected Studies" was chosen, "hepatocellular carcinoma" in cancer type was detailed, and "ARID1A" was entered as the gene. The cBioPortal source code is freely available under the GNU Lesser GPL open-source license and is hosted by Google code (http://code.google.com/p/cbio-cancergenomics-portal/).[17]

Statistical analysis

Data are presented as mean±standard deviation (SD) or standard error of the mean (SEM) from independent experiments. Statistical analyses included the Student's *t*-test and chi-squared test using GraphPad Prism 6 (GraphPad Software, Inc., La Jolla, CA, USA). A *p*-value <0.05 was considered statistically significant.

Results

ARID1A deficiency accelerates liver tumorigenesis in mice

To explore the roles of ARID1A in HCC initiation, *Arid1a* was knocked out in mice using the CRISPR/Cas9 system, as previously described.[18] A pX459 vector co-expressing a single guide (sg)RNA targeting *Arid1a* (*Arid1a* target sequence presented in Supplementary Table 1, termed sg*Arid1a*) and Cas9 was cloned. *In vitro*, sg*Arid1a* caused the loss of ARID1A in murine Hep1-6 cells (Fig. S1A). A hydrodynamic tail vein injection was used to deliver CRISPR to the livers in mice, which can affect a large proportion of hepatocytes. As shown in Figure S1B, the hydrodynamic injection of an enhanced green fluorescent protein (eGFP) plasmid DNA resulted in liver-specific expression of eGFP in mice.

First, a cohort of wild type (WT) C57BL/6 mice were administered sg*Arid1a* to determine if knockout of *Arid1a* could induce the development of tumors in the liver. Immunohistochemical (IHC) staining of liver sections using an ARID1A-specific antibody revealed that approximately 10% of hepatocytes were negative for ARID1A, but these cells were surrounded by ARID1A-positive cells (Fig. S1C). Ten months later, five sg*Arid1a*-treated mice were examined. At necropsy, zero hepatic neoplasms were noted in any of the mice (Fig. 1A).

Considering ARID1A may not directly drive liver tumorigenesis, liver damage was induced using a single intraperitoneal injection of diethylnitrosamine (DEN) at 2 weeks of age, followed by sg*Arid1a* or pX459 as control at 6 weeks of age. At 6 months, the liver phenotypes were assessed. With sg*Arid1a* treatment, four of the five mice developed hepatic tumors, whereas no tumors were found in the control group (*p*=0.048; Fig. 1B).

Considering liver tumorigenesis may result from the accumulation of multiple mutations, mice were treated simultaneously with sg*Arid1a*, sg*Pten* and sg*p53* (target sequences listed in Supplementary Table 1). Liver-specific knockout of *Pten* in mice has been shown to induce lipid accumulation and the incidence of liver cancer.[19,20] As shown in Figure S1D, knockout of *Pten* was successful, as some hepatocytes were negative for PTEN and showed signs of lipid degeneration. At 3 months, the livers were harvested from sg*Arid1a*+sg*Pten*+sg*p53* and control pX459+sg*Pten*+sg*p53* mice. There were more nodules in the livers of sg*Arid1a*+sg*Pten*+sg*p53* mice compared to the control group, although this difference did not reach statistical significance (*n*=5/group, *p*=0.067; Fig. 1C).

The above *in vivo* data suggested that ARID1A deficiency alone cannot cause liver cancer, but ARID1A may play a tumor suppressive role and its loss can accelerate liver tumorigenesis when other pro-oncogenic factors are introduced.

ARID1A mutations are associated with a poorer prognosis in HCC patients

To dissect the function of *ARID1A* in HCC patients, a human survival analysis was conducted using cBioPortal (https://www.cbioportal.org/)[17,21] with data from TCGA Liver Hepatocellular Carcinoma (source data from GDAC Firehose). Thirty-four mutations of *ARID1A* were observed in 32 HCC patients (specific mutations listed in Supplementary Table 4). The results of the Kaplan-Meier survival analysis suggested that patients with an *ARID1A* mutation had a poor prognosis in terms of overall survival (*n*=365, *p*=0.008093); however, there was no significant difference in disease-free survival (*n*=315, *p*=0.0719; Fig. 2A). Interestingly, the human clinical survey showed that patients with an *ARID1A* mutation had more adjacent hepatic tissue inflammation compared to those with WT *ARID1A* (*p*=0.002194, *q*=0.0757; Fig. 2B).

Next, expression profiling analysis was performed based on the subset data of TCGA Liver Hepatocellular Carcinoma. Expression profiles of mRNA were displayed using a volcano plot (Fig. 2C). A total of 216 differentially expressed genes are listed in Supplementary Table 5. The mRNA levels of *MYC*, a known oncogene, were significantly higher in the *ARID1A* mutation group compared to the WT *ARID1A* group (*p*=9.28 e−8, *q*=1.332 e−4; Fig. 2D).

In summary, these human clinical results revealed that an *ARID1A* mutation was associated with poorer prognosis in HCC patients. *MYC* was a candidate gene that is regulated by ARID1A, which may exert its tumor suppressive functions.

ARID1A inhibits HCC cell proliferation and is required for DNA damage repair and apoptosis

To study the function of ARID1A *in vitro*, the expression levels of ARID1A were first detected in a variety of HCC cell lines. Using western blot analysis, Bel7404 and HepG2 cells were found to be "ARID1A-positive". In contrast, Huh7 cells were "ARID1A-negative" (Fig. 3A). To test whether ARID1A

Fig. 1. ARID1A deficiency accelerates liver tumorigenesis in mice. (A) Knockout of *Arid1a* alone in C57BL/6 mice using the CRISPR/Cas9 system did not cause liver cancer (*n*=5). (B) Knockout of *Arid1a* in C57BL/6 mice previously exposed to DEN can accelerate liver tumorigenesis (*n*=5/group, *p*=0.048). Arrows indicate liver tumors. (C) C57BL/6 mice were injected with sg*Pten*+sg*p53*+sg*Arid1a* or sg*Pten*+sg*p53* (control). Nodules formed in the sg*Pten*+sg*P53*+sg*Arid1a* group and the sg*Pten*+sg*P53* group (*n*=5/group, *p*=0.067). Arrows indicate liver nodules. ARID1A, AT-rich interactive domain-containing protein 1A; CRISPR/Cas9, clustered regularly interspaced short palindrome repeats/CRISPR-associated protein 9; DEN, diethylnitrosamine.

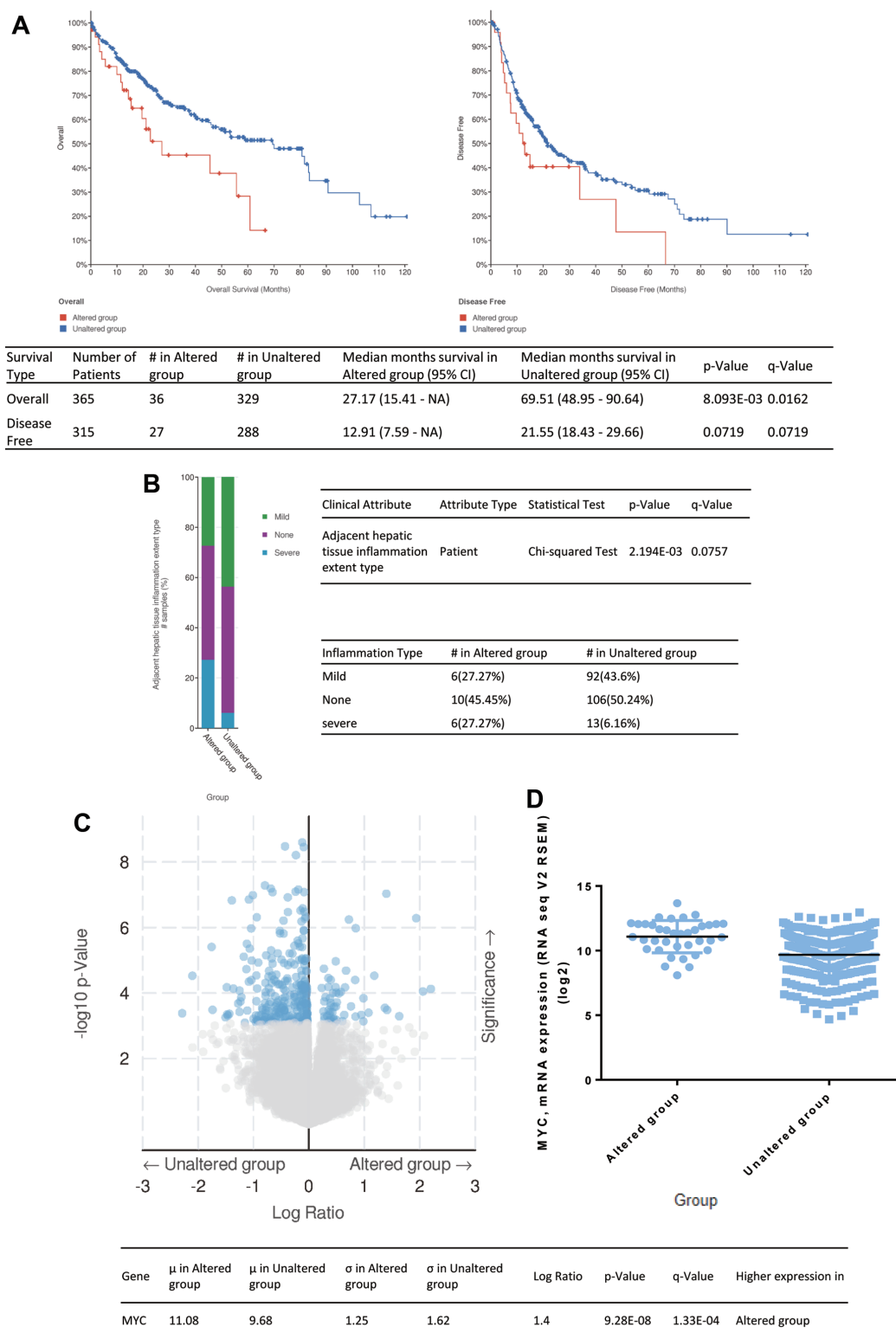| Survival Type	Number of Patients	# in Altered group	# in Unaltered group	Median months survival in Altered group (95% CI)	Median months survival in Unaltered group (95% CI)	p-Value	q-Value
Overall	365	36	329	27.17 (15.41 - NA)	69.51 (48.95 - 90.64)	8.093E-03	0.0162
Disease Free	315	27	288	12.91 (7.59 - NA)	21.55 (18.43 - 29.66)	0.0719	0.0719

Clinical Attribute	Attribute Type	Statistical Test	p-Value	q-Value
Adjacent hepatic tissue inflammation extent type	Patient	Chi-squared Test	2.194E-03	0.0757

Inflammation Type	# in Altered group	# in Unaltered group
Mild	6(27.27%)	92(43.6%)
None	10(45.45%)	106(50.24%)
severe	6(27.27%)	13(6.16%)

Gene	μ in Altered group	μ in Unaltered group	σ in Altered group	σ in Unaltered group	Log Ratio	p-Value	q-Value	Higher expression in
MYC	11.08	9.68	1.25	1.62	1.4	9.28E-08	1.33E-04	Altered group

Fig. 2. An *ARID1A* mutation was associated with a poorer prognosis in HCC patients. (A) Kaplan-Meier survival analysis (data from TCGA, Firehose Legacy) using cBioPortal suggested that patients with an *ARID1A* mutation had a poor prognosis regarding overall survival (n=365, p=8.093 e−03) but no significant difference in disease-free survival (n=315, p=0.0719). (B) HCC patients with an *ARID1A* mutation had more adjacent hepatic tissue inflammation (p=2.194e−03). (C) Volcano plot of the differential expression of mRNAs between HCC patients with an *ARID1A* mutation and those with WT *ARID1A*. (D) mRNA expression of MYC was significantly higher in HCC patients with an *ARID1A* mutation (p=9.28 e−8, q=1.332 e−4). ARID1A, AT-rich interactive domain-containing protein 1A; HCC, hepatocellular carcinoma; TCGA, The Cancer Genome Atlas.
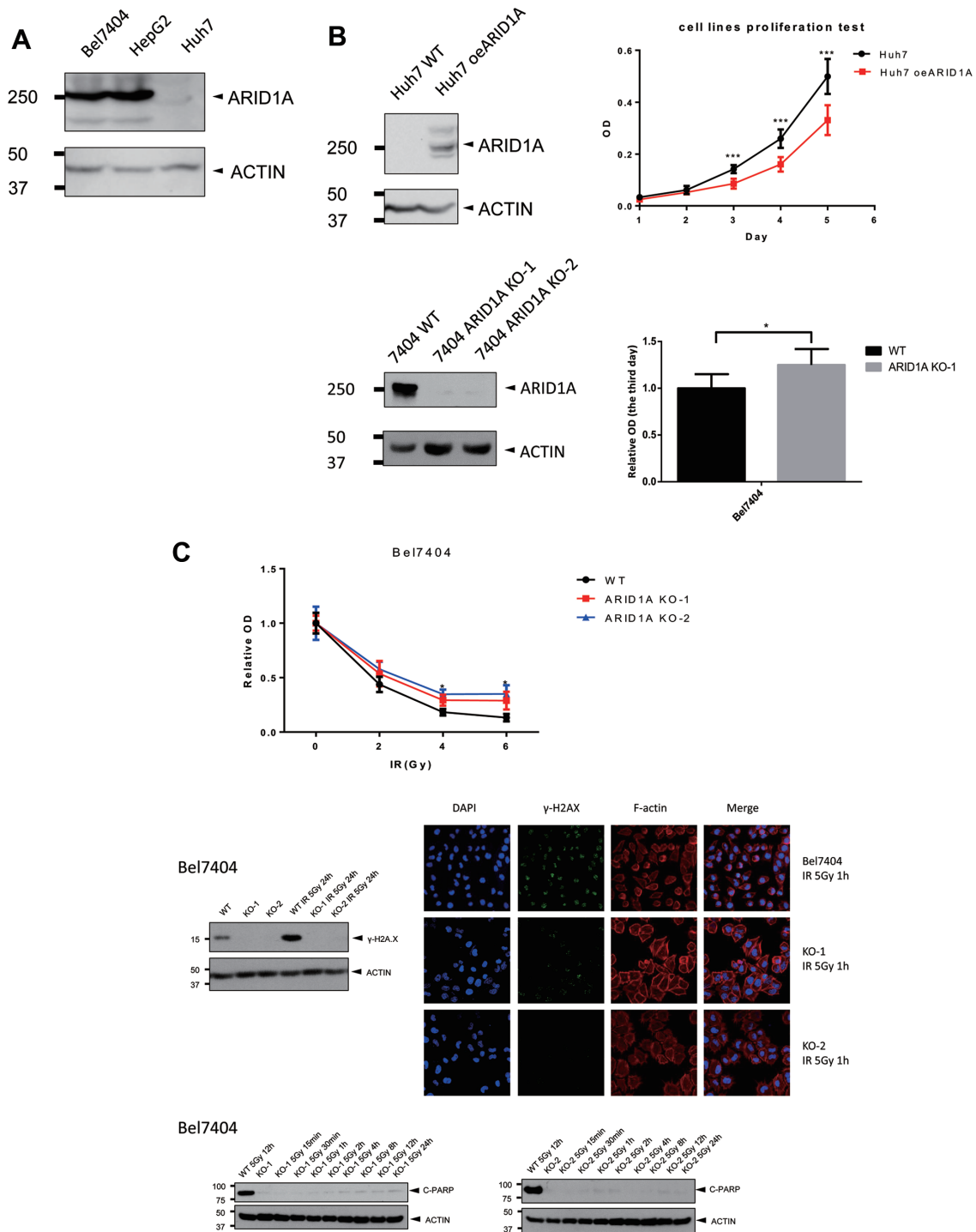
Fig. 3. ARID1A inhibits HCC cell proliferation, DNA damage repair and apoptosis. (A) Western blotting revealed protein expression level of ARID1A and actin in different HCC cell lines. (B) Huh7 cells were stably infected with a lentivirus expressing ARID1A cDNA for overexpression or ARID1A (above left). Bel7404 cells were transiently transfected with Cas9 and sg*ARID1A* and two randomly chosen monoclonal *ARID1A* knockout cell lines (KO-1, KO-2; lower left) were used for subsequent experiments. The MTT assay was performed to determine cell proliferation capacity (above right, below right). Experiments were performed in triplicate. Quantification data are presented as mean±SD. *$p<0.05$, ***$p<0.001$. (C) WT and ARID1A knockout Bel7404 cells were treated with radiation (0, 2, 4, 6 Gy, respectively). The MTT assay was performed to determine cell viability (above). Experiments were performed in triplicate. Quantification data are presented as mean±SD. *$p<0.05$. WT and ARID1A knockout Bel7404 cells were treated with 5 Gy IR. Twenty-four hours after radiation, γ-H2AX and actin were detected by western blot (middle left). One hour after radiation, γ-H2AX, DAPI and F-actin were detected by IF (middle right). WT and *ARID1A* knockout Bel7404 cells were treated with 5 Gy IR. The protein levels of c-PARP and actin at various time points were detected using western blotting. ARID1A, AT-rich interactive domain-containing protein 1A; c-PARP, cleaved poly (ADP-ribose) polymerase; DAPI, 4',6-diamidino-2-phenylindole; HCC, hepatocellular carcinoma; KO, knockout; MTT, 3-(4,5-dimethylthiazol-2-yl)-2,5-diphenyl-2H-tetrazolium bromide; SD, standard deviation; WT, wild type; γ-H2AX, gamma histone 2 A variant X.
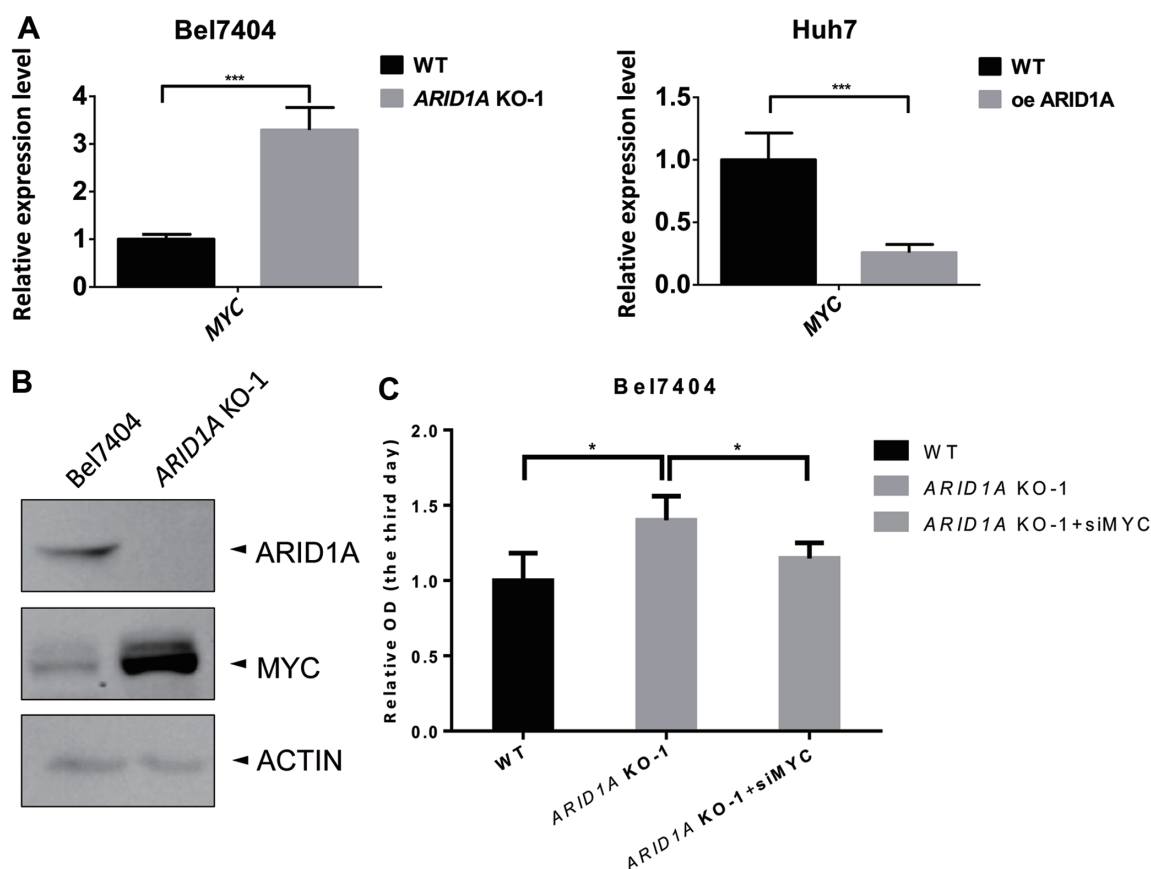
Fig. 4. ARID1A inhibits HCC cell proliferation via down-regulation of MYC transcription. (A) In WT and *ARID1A* knockout Bel7404 cells (left), WT Huh7 cells and those with over expressed ARID1A (right), the differential mRNA levels of MYC were detected using qPCR. Experiments were performed in triplicate. Quantification data are presented as mean±SD. ***$p<0.001$. (B) In WT and ARID1A knockout Bel7404 cells, the protein levels of MYC were detected by western blot. (C) ARID1A knockout Bel7404 cells were transfected with siMYC. The proliferation capacity of WT, ARID1A knockout and ARID1A knockout plus siMYC Bel7404 cells was detected using an MTT assay. Experiments were performed in triplicate. Quantitation data are presented as mean±SD. *$p<0.05$. si, small interfering RNA. ARID1A, AT-rich interactive domain-containing protein 1A; HCC, hepatocellular carcinoma; MTT, 3-(4,5-dimethylthiazol-2-yl)-2,5-diphenyl-2H-tetrazolium bromide; qPCR, quantitative reverse-transcription polymerase chain reaction; SD, standard deviation; WT, wild type.

is crucial for HCC cell proliferation, ARID1A was further manipulated and the proliferation of HCC cells was examined using a MTT assay. The results revealed that overexpression of ARID1A in Huh7 cells inhibited their proliferation and knockout of ARID1A in Bel7404 cells (ARID1A KO cells) resulted in enhanced proliferation (Fig. 3B).

Next, the cellular responses to DNA damage were investigated. An MTT assay revealed better cell viability in ARID1A KO cells after ionizing radiation (IR) treatment, suggesting that the knockout of ARID1A in HCC cells caused the cells to become more resistant to IR stress (Fig. 3C, top). Results from western blot and immunofluorescence (IF) assays revealed that ARID1A KO cells could not accumulate the same level of gamma histone 2 A variant X after radiation treatment compared to WT Bel7404 cells (Fig. 3C, middle). Results from the apoptosis assay, where cleaved poly (ADP-ribose) polymerase (c-PARP) was detected by western blotting, also revealed that knockout of ARID1A could dramatically decrease the levels of c-PARP after IR treatment (Fig. 3C, bottom), suggesting that the tumor suppressive role of ARID1A could be the result of inducing apoptosis in damaged cells.

Taken together, the above data suggest that ARID1A inhibits HCC cell proliferation and is required for DNA damage repair and apoptosis.

ARID1A inhibits cell proliferation of HCC cells via downregulation of MYC transcription

Expression profiles of mRNA indicated that MYC might contribute to the ARID1A-dependent regulation of cell proliferation. To test this hypothesis concerning the molecular mechanism, transcript levels of MYC were detected using qPCR. Consistent with the gene expression profiling analysis, knockout of ARID1A increased the level of MYC mRNA in Bel7404 cells, while overexpression of ARID1A resulted in a decrease of MYC mRNA in Huh7 cells (Fig. 4A). Using western blotting, knockout of ARID1A increased the level of MYC protein in Bel7404 cells (Fig. 4B). In addition, knockdown of MYC in Bel7404 cells could reverse the proproliferative effect caused by knockout of ARID1A (Fig. 4C).

Taken together, these data presented in Figure 4 suggest that MYC can be regulated by ARID1A and this contributes to the regulation of cell proliferation.

Discussion

HCC is one of the most common types of liver cancer, and accounts for 90% of all primary liver cancers.[22] However, effective treatments for HCC are lacking due to its het-

erogeneity.[23] HCC patients carry mutations in numerous genes, including *ARID1A*. In the TCGA data set, 8.22% (30/365) of HCC patients carry an *ARID1A* mutation, and most of these are inactivating mutations. The clinicopathologic significance of ARID1A expression in HCC has been investigated previously, and it was revealed that 12.17% of HCC tumors (14/115) were ARID1A-negative and that loss of ARID1A was significantly associated with larger tumors.[24]

In this study, the knockout of *Arid1a* alone could not initiate liver cancer in mice, suggesting that it is not a cancer-driver gene. However, knockout of *Arid1a* accelerated liver tumorigenesis when DEN or a combination knockout of *Pten* and *p53* were introduced, suggesting that liver tumorigenesis is a multistep process that requires various other factors. Similar results have been reported by others, such as the finding of mice with homozygous or heterozygous deletions in *Arid1a* not developing ovarian lesions but mice with an *Arid1a* and *Pten* double-knockout developing ovarian endometrioid cancer.[25]

Further TCGA data analysis showed that *ARID1A* mutations are associated with a poorer prognosis in HCC patients, indicating that ARID1A may have prognostic value. Expression profiles of mRNA showed that *MYC* transcription was significantly higher in patients with an *ARID1A* mutation. *ARID1A* mutations resulted in abnormal chromatin remodeling that diverted gene transcription. Previously, others have also reported that mutant ARID1A is able to promote cell proliferation by triggering the phosphoinositide 3-kinase/protein kinase B (PI3K/AKT) signaling pathway,[26,27] which affects the expression of other cell cycle regulators, such as the *MYC* gene.[28] Consistent with previous reports, the contribution of MYC to the antiproliferative effect of ARID1A in HCC was definitively shown in the present study.

The role of ARID1A in DNA damage repair and apoptosis was also investigated. ARID1A knockout resulted in disruptions of DNA damage repair and apoptosis following IR exposure. Loss of ARID1A led to disrupted SWI/SNF function, which caused enhanced mutagenesis due to the defective DNA repair and aberrant apoptosis evasion.[29,30] Thus, tumorigenesis of HCC with an *ARID1A* mutation is complex and involves an intricate network of mechanisms, including cell proliferation, DNA damage repair and apoptosis signaling pathways.

Undoubtedly, the full decoding of the ARID1A tumor suppressive mechanism may have future therapeutic implications. These data support the role of ARID1A in protection against HCC progression. Several targeted therapy drugs should also be considered in future studies, including inhibitors of MYC or PI3K/AKT signaling, PARP inhibitors targeting the DNA damage signaling pathway, and synthetic lethal therapies targeting epigenetic changes in *ARID1A* mutation-based cancers. Interestingly, it was also shown that patients with an *ARID1A* mutation had more severe adjacent hepatic tissue inflammation, suggesting that ARID1A is involved in tumor immunity and may be targeted by immunotherapy.

In summary, the current findings further elucidate the tumor-suppressive mechanism of ARID1A in HCC. A loss-of-function *ARID1A* mutation promotes cell proliferation and disrupts DNA damage repair and apoptosis pathways. Loss of ARID1A may promote HCC progression via the transcriptional up-regulation of MYC.

Acknowledgments

Conflict of interest

The authors have no conflict of interests related to this publication.

Author contributions

Study concept and design (JZ, YX), acquisition of data (JZ, YX, GL, XO, DZ), analysis and interpretation of data (JZ, YX, GL, JxZ, XL, QZ), drafting of the manuscript (JZ, YX), critical revision of the manuscript for important intellectual content (JZ, YX), administrative, technical, or material support, study supervision (JZ).

Data sharing statement

No additional data are available.

References

[1] Waller LP, Deshpande V, Pyrsopoulos N. Hepatocellular carcinoma: a comprehensive review. World J Hepatol 2015;7(26):2648–2663. doi:10.4254/wjh.v7.i26.2648.
[2] Alqahtani A, Khan Z, Alloghbi A, Said Ahmed TS, Ashraf M, Hammouda DM. Hepatocellular carcinoma: molecular mechanisms and targeted therapies. Medicina (Kaunas) 2019;55(9):526. doi:10.3390/medicina55090526.
[3] Cancer Genome Atlas Research Network. Comprehensive and integrative genomic characterization of hepatocellular carcinoma. Cell 2017; 169(7):1327–1341.e23. doi:10.1016/j.cell.2017.05.046.
[4] Schulze K, Nault JC, Villanueva A. Genetic profiling of hepatocellular carcinoma using next-generation sequencing. J Hepatol 2016;65(5):1031–1042. doi:10.1016/j.jhep.2016.05.035.
[5] Ding XX, Zhu QG, Zhang SM, Guan L, Li T, Zhang L, et al. Precision medicine for hepatocellular carcinoma: driver mutations and targeted therapy. Oncotarget 2017;8(33):55715–55730. doi:10.18632/oncotarget.18382.
[6] Abe H, Hayashi A, Kunita A, Sakamoto Y, Hasegawa K, Shibahara J, et al. Altered expression of AT-rich interactive domain 1A in hepatocellular carcinoma. Int J Clin Exp Pathol 2015;8(3):2763–2770.
[7] Nair SS, Kumar R. Chromatin remodeling in cancer: a gateway to regulate gene transcription. Mol Oncol 2012;6(6):611–619. doi:10.1016/j.molonc.2012.09.005.
[8] Wu RC, Wang TL, Shih Ie M. The emerging roles of ARID1A in tumor suppression. Cancer Biol Ther 2014;15(6):655–664. doi:10.4161/cbt.28411.
[9] Klapproth K, Wirth T. Advances in the understanding of MYC-induced lymphomagenesis. Br J Haematol 2010;149(4):484–497. doi:10.1111/j.1365-2141.2010.08159.x.
[10] Dang CV. MYC on the path to cancer. Cell 2012;149(1):22–35. doi:10.1016/j.cell.2012.03.003.
[11] Kalkat M, De Melo J, Hickman KA, Lourenco C, Redel C, Resetca D, et al. MYC deregulation in primary human cancers. Genes (Basel) 2017;8(6):151. doi:10.3390/genes8060151.
[12] Kawate S, Fukusato T, Ohwada S, Watanuki A, Morishita Y. Amplification of c-myc in hepatocellular carcinoma: correlation with clinicopathologic features, proliferative activity and p53 overexpression. Oncology 1999;57(2):157–163. doi:10.1159/000012024.
[13] Schlaeger C, Longerich T, Schiller C, Bewerunge P, Mehrabi A, Toedt G, et al. Etiology-dependent molecular mechanisms in human hepatocarcinogenesis. Hepatology 2008;47(2):511–520. doi:10.1002/hep.22033.
[14] Li L, Jin R, Zhang X, Lv F, Liu L, Liu D, et al. Oncogenic activation of glypican-3 by c-Myc in human hepatocellular carcinoma. Hepatology 2012; 56(4):1380–1390. doi:10.1002/hep.25891.
[15] Liu P, Ge M, Hu J, Li X, Che L, Sun K, et al. A functional mammalian target of rapamycin complex 1 signaling is indispensable for c-Myc-driven hepatocarcinogenesis. Hepatology 2017;66(1):167–181. doi:10.1002/hep.29183.
[16] Cong L, Ran FA, Cox D, Lin S, Barretto R, Habib N, et al. Multiplex genome engineering using CRISPR/Cas systems. Science 2013;339(6121):819–823. doi:10.1126/science.1231143.
[17] Cerami E, Gao J, Dogrusoz U, Gross BE, Sumer SO, Aksoy BA, et al. The cBio cancer genomics portal: an open platform for exploring multidimensional cancer genomics data. Cancer Discov 2012;2(5):401–404. doi:10.1158/

2159-8290.CD-12-0095.

[18] Xue W, Chen S, Yin H, Tammela T, Papagiannakopoulos T, Joshi NS, *et al*. CRISPR-mediated direct mutation of cancer genes in the mouse liver. Nature 2014;514(7522):380–384. doi:10.1038/nature13589.

[19] Horie Y, Suzuki A, Kataoka E, Sasaki T, Hamada K, Sasaki J, *et al*. Hepatocyte-specific Pten deficiency results in steatohepatitis and hepatocellular carcinomas. J Clin Invest 2004;113(12):1774–1783. doi:10.1172/JCI20513.

[20] Stiles B, Wang Y, Stahl A, Bassilian S, Lee WP, Kim YJ, *et al*. Liver-specific deletion of negative regulator Pten results in fatty liver and insulin hypersensitivity [corrected]. Proc Natl Acad Sci U S A 2004;101(7):2082–2087. doi:10.1073/pnas.0308617100.

[21] Gao J, Aksoy BA, Dogrusoz U, Dresdner G, Gross B, Sumer SO, *et al*. Integrative analysis of complex cancer genomics and clinical profiles using the cBioPortal. Sci Signal 2013;6(269):pl1. doi:10.1126/scisignal.2004088.

[22] Siegel RL, Miller KD, Jemal A. Cancer statistics, 2019. CA Cancer J Clin 2019;69(1):7–34. doi:10.3322/caac.21551.

[23] Wang XW, Thorgeirsson SS. The biological and clinical challenge of liver cancer heterogeneity. Hepat Oncol 2014;1(4):349–353. doi:10.2217/hep.14.18.

[24] Zhao J, Chen J, Lin H, Jin R, Liu J, Liu X, *et al*. The clinicopathologic significance of BAF250a (ARID1A) expression in hepatocellular carcinoma. Pathol

Oncol Res 2016;22(3):453–459. doi:10.1007/s12253-015-0022-9.

[25] Guan B, Rahmanto YS, Wu RC, Wang Y, Wang Z, Wang TL, *et al*. Roles of deletion of Arid1a, a tumor suppressor, in mouse ovarian tumorigenesis. J Natl Cancer Inst 2014;106(7):dju146. doi:10.1093/jnci/dju146.

[26] Lee D, Yu EJ, Ham IH, Hur H, Kim YS. AKT inhibition is an effective treatment strategy in ARID1A-deficient gastric cancer cells. Onco Targets Ther 2017;10:4153–4159. doi:10.2147/OTT.S139664.

[27] Bosse T, ter Haar NT, Seeber LM, v Diest PJ, Hes FJ, Vasen HF, *et al*. Loss of ARID1A expression and its relationship with PI3K-Akt pathway alterations, TP53 and microsatellite instability in endometrial cancer. Mod Pathol 2013;26(11):1525–1535. doi:10.1038/modpathol.2013.96.

[28] Nagl NG Jr, Wang X, Patsialou A, Van Scoy M, Moran E. Distinct mammalian SWI/SNF chromatin remodeling complexes with opposing roles in cell-cycle control. EMBO J 2007;26(3):752–763. doi:10.1038/sj.emboj.7601541.

[29] Shen J, Peng Y, Wei L, Zhang W, Yang L, Lan L, *et al*. ARID1A deficiency impairs the DNA damage checkpoint and sensitizes cells to PARP inhibitors. Cancer Discov 2015;5(7):752–767. doi:10.1158/2159-8290.CD-14-0849.

[30] Helming KC, Wang X, Roberts CWM. Vulnerabilities of mutant SWI/SNF complexes in cancer. Cancer Cell 2014;26(3):309–317. doi:10.1016/j.ccr.2014.07.018.